PHYSICAL REVIEW A **102**, 032816 (2020)

Parity-nonconserving interactions of electrons in chiral molecules with cosmic fields

Konstantin Gaul,[1] Mikhail G. Kozlov,[2,3] Timur A. Isaev,[2] and Robert Berger[1]
[1]*Fachbereich Chemie, Philipps-Universität Marburg, Hans-Meerwein-Straße 4, 35032 Marburg, Germany*
[2]*Petersburg Nuclear Physics Institute of NRC "Kurchatov Institute," Gatchina 188300, Russia*
[3]*St. Petersburg Electrotechnical University "LETI," Professor Popov Street 5, 197376 St. Petersburg, Russia*

(Received 11 May 2020; accepted 12 August 2020; published 16 September 2020)

Parity ($\mathcal{P}$)–violating pseudoscalar or pseudovector cosmic fields are invoked in different models for cold dark matter or in the standard model extension that allows for Lorentz invariance violation. A direct detection of the timelike component of such fields requires a direct measurement of $\mathcal{P}$-odd potentials or their evolution over time. Herein, advantageous properties of chiral molecules, in which $\mathcal{P}$-odd potentials lead to resonance frequency differences between enantiomers, for direct detection of such $\mathcal{P}$-odd cosmic field interactions are demonstrated. Scaling behavior of electronic structure enhancements of such interactions with respect to nuclear charge number and the fine-structure constant is derived analytically. This allows a simple estimate of the effect sizes for arbitrary molecules. The analytical derivation is supported by quasirelativistic numerical calculations in the molecules H_2X_2 and H_2XO with $X = \mathrm{O}$, S, Se, Te, or Po. Parity-violating effects due to cosmic fields on the C–F stretching mode in CHBrClF are compared to electroweak parity violation and influences of nonseparable anharmonic vibrational corrections are discussed. On this basis, Gaul *et al.* [Phys. Rev. Lett. **125**, 123004 (2020)] estimated from a 20-year-old experiment with CHBrClF that bounds on Lorentz invariance violation as characterized by the parameter $|b_0^{\mathrm{e}}|$ can be pushed down to the order of 10^{-17} GeV in modern experiments with suitably selected molecular system, which will be an improvement of the current best limits by at least two orders of magnitude. This serves to highlight the particular opportunities that precision spectroscopy of chiral molecules provides in the search for new physics beyond the standard model.

DOI: 10.1103/PhysRevA.102.032816

I. INTRODUCTION

In our recent work [1], the virtues and prospects of chiral molecules as direct sensors for pseudovector and pseudoscalar cosmic fields were demonstrated. In the present paper, we derive scaling laws for interactions of electrons with these fields, presented in Ref. [1], and provide support from numerical calculations. Furthermore, the methods applied for derivation of limits on cosmic field interactions from experiments with chiral molecules are presented in a more detailed manner and accompanied by comparison to other computational methods.

One of the biggest puzzles of modern physics is the nature and composition of dark matter (DM) (see, e.g., Ref. [2]). Many different models for DM exist, considering objects that range from macroscopic to microscopic and from being hot (ultrarelativistic) to cold (nonrelativistic). Among these DM theories, cold DM (CDM) theory serves to provide a simple explanation for many cosmological observations [3]. However, the constituents of CDM are unknown and can in principle fall in the range from macroscopic objects such as black holes to new fundamental particles like weakly interacting massive particles (WIMPs), axions, sterile neutrinos, or dark photons (see, e.g., Refs. [4–6]).

Despite its merits, the model of CDM has several drawbacks [7–12]. Notable challenges are the cusps of halos in CDM simulations, which are not observed in rotation curves of galaxies [7], or the prediction of a large number of nonobserved halos of CDM [8]. A possible solution of some of these, such as the large number of absent halos or cusps of halos is provided by fuzzy CDM models [13]. Fuzzy CDM is supposed to consist of ultralight particles with masses of $m_\phi \approx 1 \times 10^{-22}\,\mathrm{eV}/c^2$ [13,14]. This model makes searches for ultralight CDM oscillating with frequencies on the order of $1\,\mu$Hz particularly interesting.

CDM can consist of various types of bosons (an overview can be found, e.g., in Ref. [15]). Among those, pseudoscalar and pseudovector fields are of special interest as they are a source of parity ($\mathcal{P}$) violation.

Pseudoscalar CDM particles behave like axions, which were originally proposed [16–18] to solve the strong $\mathcal{CP}$ problem of quantum chromodynamics (QCD) [19]. The search for CDM particles can be restricted to a comparatively small parameter space assessable to the QCD axion (see, e.g., Ref. [20]) or can involve a wide range for axionic particles that are not bound to solve the strong $\mathcal{CP}$ problem. The latter are often referred to as axionlike particles (ALPs). *Pseudovector* fields are important for models such as dark photons [21,22] and also appear as sources of local Lorentz invariance violation in the standard model extension (SME) by Kostelecký and coworkers [23].

In the past decade, many proposals for experiments and improved bounds on pseudoscalar CDM appeared, employing atomic spectroscopy (see, e.g., Refs. [24–29]). Among those, strict limits on static $\mathcal{P}$-odd field interactions were set from direct detection of $\mathcal{P}$ violation with modern atomic precision spectroscopy [27,30]. In these experiments, the dominating effect for $\mathcal{P}$ violation stems from the electroweak Z^0-mediated electron-nuclear interaction.

Such $\mathcal{P}$-odd effects are strongly enhanced in chiral molecules as well (for recent reviews on molecular $\mathcal{P}$ violation, see Refs. [31–37]). The chiral arrangement of the nuclei in the molecule leads to helicity of the electron cloud (see, e.g., Ref. [36]). Additional $\mathcal{P}$-odd effects can then be measured as energy difference between enantiomers of chiral molecules or as resonance frequency differences between the two nonidentical mirror-image molecules [38–40]. As frequency shifts can be measured very accurately (see, e.g., Ref. [41] or for the special case of $\mathcal{P}$ violation, see Refs. [42,43]), this appears to be a particularly promising tool to search for $\mathcal{P}$-odd cosmic field interactions.

In the following, we analyze in detail the effects that emerge from $\mathcal{P}$-odd cosmic field interactions in chiral molecules. We derive scaling laws with respect to nuclear charge and the fine structure constant and compare to what is known from $\mathcal{P}$ violation due to electroweak interactions. From our analysis, we demonstrate advantages of the use of chiral molecules to search for $\mathcal{P}$-odd cosmic field interactions. We perform quasirelativistic calculations at different levels of theory and estimate the effect sizes in the vibrational spectra of the chiral methane derivate CHBrClF [44,45]. Thereby, the computational difficulties are highlighted. From a 20-year-old experiment with this molecule [46], we estimated the sensitivity on cosmic $\mathcal{P}$ violation [1] and discuss the scope for improvement on these limits in modern experiments with chiral molecules and by improvement of the present theoretical methods.

II. THEORY

A. Parity-nonconserving interactions of electrons with cosmic fields

$\mathcal{P}$-odd interactions of electrons with pseudoscalar and pseudovector cosmic fields were discussed in detail in Ref. [30]. A light pseudoscalar cosmic field obeys the Klein-Gordon equation. Assuming it to be nonrelativistic, i.e., $\hbar\omega_\phi \approx m_\phi c^2$ with m_ϕ being the CDM particle mass and c being the speed of light in vacuum, we can write

$$\phi(\vec{r},t) = \phi_0 \cos\left(\omega_\phi t - \frac{\vec{r}\cdot\vec{p}_\phi}{\hbar} + \varphi\right), \tag{1}$$

where $\hbar = \frac{h}{2\pi}$ is the reduced Planck's constant, ϕ_0 is the CDM amplitude, $\vec{p}_\phi = m_\phi \vec{v}_\phi$ is the momentum of the CDM particle, which is proportional to its velocity $\vec{v}_\phi$, and φ is a phase factor. CDM is supposed to be incoherent and the relative velocity of the ALP field is suppressed by 10^{-3} with respect to the speed of light (see Refs. [24,25] for details). Thus, for terrestrial experiments, we can assume $\frac{\vec{r}\cdot\vec{p}_\phi}{\hbar}$ to be constant and choose φ such that Eq. (1) can be written as $\phi(\vec{r},t) = \phi_0\cos(\omega_\phi t)$ (see also Ref. [30]).

The interaction of the electronic field ψ_e with such pseudoscalar fields ϕ can be described by (see, e.g., Refs. [17,18])

$$\mathcal{L}^{\phi}_{\mathrm{ps}} = g_{\phi\bar{\mathrm{e}}\mathrm{e}}(\hbar c\,\partial_\mu\phi)\bar{\psi}_\mathrm{e}\boldsymbol{\gamma}^\mu\boldsymbol{\gamma}^5\psi_\mathrm{e}\,, \tag{2}$$

where $g_{\phi\bar{\mathrm{e}}\mathrm{e}}$ is a coupling constant of dimension GeV^{-1}. Herein the Dirac matrices are defined as

$$\boldsymbol{\gamma}^0 = \begin{pmatrix} \mathbf{1}_{2\times2} & \mathbf{0}_{2\times2} \\ \mathbf{0}_{2\times2} & -\mathbf{1}_{2\times2} \end{pmatrix}, \quad \boldsymbol{\gamma}^k = \begin{pmatrix} \mathbf{0}_{2\times2} & \boldsymbol{\sigma}^k \\ -\boldsymbol{\sigma}^k & \mathbf{0}_{2\times2} \end{pmatrix}, \tag{3}$$

where $\boldsymbol{\sigma}^k$ are the Pauli spin matrices, $k = 1,2,3$, and $\mu = 0,1,2,3$. $\boldsymbol{\gamma}^5 = \imath\boldsymbol{\gamma}^0\boldsymbol{\gamma}^1\boldsymbol{\gamma}^2\boldsymbol{\gamma}^3$, where $\imath = \sqrt{-1}$ is the imaginary unit, $\partial_\mu = \frac{\partial}{\partial x^\mu}$ is the first derivative with respect to the four-vector $x^\mu = (ct, x, y, z)$ and Einstein's sum convention is used. Additionally a direct pseudoscalar coupling between the electrons and the pseudoscalar cosmic field can be considered (see, e.g., Ref. [27]):

$$\mathcal{L}^{\phi}_{\mathrm{dps}} = -\imath\tilde{g}_{\phi\bar{\mathrm{e}}\mathrm{e}} m_\mathrm{e} c^2 \phi\bar{\psi}_\mathrm{e}\boldsymbol{\gamma}^5\psi_\mathrm{e}\,, \tag{4}$$

where $\tilde{g}_{\phi\bar{\mathrm{e}}\mathrm{e}}$ is a dimensionless coupling constant and m_e is the mass of the electron. Whereas this interaction can lead to $\mathcal{P}$-violating couplings when considering transition matrix elements of atomic or molecular excitations [30], it does not contribute to $\mathcal{P}$-violating expectation values, which give dominant contributions to frequency differences in spectra of chiral molecules. Thus, these interactions are not discussed any further in the following.

The time derivative of the pseudoscalar field leads to the $\mathcal{P}$-odd single-electron Hamiltonian

$$\hat{h}_{\mathrm{ps}} = g_{\phi\bar{\mathrm{e}}\mathrm{e}}\sqrt{2(hc)^3\rho_{\mathrm{CDM}}}\,\sin(\omega_\phi t)\boldsymbol{\gamma}^5, \tag{5}$$

where $\rho_{\mathrm{CDM}} \approx \frac{(\hbar\omega_\phi\phi_0)^2}{2(hc)^3}$ is the CDM energy density, for which we assume all ALPs to comprise all of the CDM with a uniform density: $(hc)^3\rho_{\mathrm{CDM}} = (hc)^3 0.4\,\mathrm{GeV\,cm^{-3}} = 7.6\times10^{-4}\,\mathrm{eV}^4$ (see Ref. [47]). We use lowercase letters ($\hat{h}$) for single-electron operators and uppercase letters ($\hat{H}$) for multielectron operators. These are in the case of $\hat{H}_{\mathrm{ps}}$ (as well as $\hat{H}_{\mathrm{pv}}$, $\hat{H}_{\mathrm{ew}}$ given below) simple sums over all electrons of the system, e.g., $\hat{H}_{\mathrm{ps}} = \sum_i \hat{h}_{\mathrm{ps}}(i)$.

Electronic interactions with pseudovector cosmic fields can be described by the Lagrangian

$$\mathcal{L}^{b}_{\mathrm{pv}} = -b_\mu\bar{\psi}_\mathrm{e}\boldsymbol{\gamma}^\mu\boldsymbol{\gamma}^5\psi_\mathrm{e}, \tag{6}$$

which appears, e.g., in the SME (for details, see Refs. [23,48]).

The parity-nonconserving interaction Hamiltonian for the temporal component is

$$\hat{h}_{\mathrm{pv}} = b_0(t)\boldsymbol{\gamma}^5, \tag{7}$$

where the field can be static $b_0(t) = b^\mathrm{e}_0$ or dynamic $b^\mathrm{e}_0(t) = b^\mathrm{e}_0\sin(\omega_b t)$. Here b^e_0 is the interaction strength of the timelike component of the pseudovector field with the electrons.

In spectra of chiral molecules, the interactions discussed above lead to shifts (static fields) or oscillations (dynamic fields) of frequency shifts due to the nuclear spin-independent electroweak interactions, the main contribution to which is in closed-shell molecules expected to arise from the electron-nuclei weak neutral-current interaction Hamiltonian (see, e.g., Refs. [31,32]):

$$\hat{h}_{\mathrm{ew}} = \frac{G_{\mathrm{F}}}{2\sqrt{2}} \sum_{A=1}^{N_{\mathrm{nuc}}} Q_{\mathrm{W},A}\, \rho_A(\vec{r})\boldsymbol{\gamma}^5 \,, \tag{8}$$

where $G_{\mathrm{F}} = 2.22249 \times 10^{-14} E_h a_0^3$ is Fermi's weak coupling constant and $Q_{\mathrm{W},A}$ and ρ_A are the weak charge and normalized charge density of nucleus A, respectively. The total number of nuclei is N_{nuc}. Contributions from $\mathcal{P}$-odd nuclear-spin-dependent terms when combined with $\mathcal{P}$-even hyperfine coupling [49,50] are estimated to give only minor contributions in closed-shell molecules. Similar considerations hold for the contribution from neutral-current interaction terms between electrons.

It shall be noted that in chiral molecules weakly interacting dark matter candidates, such as WIMPs, or cosmic neutrinos can also lead to shifts or oscillations of the $\mathcal{P}$-odd potential as was discussed by Bargueño *et al.* [51–53]. These interactions as well as those of electrons with pseudoscalar and pseudovector fields discussed above are proportional to $\langle \boldsymbol{\gamma}^5 \rangle$. In the following, we will discuss in general the chiral operator $\boldsymbol{\gamma}^5$, which leads to parity nonconservation and compare it to known properties of operator Eq. (8).

B. Molecular expectation value of $\boldsymbol{\gamma}^5$

The time-independent Dirac-Coulomb equation for the electronic system of the molecule reads

$$\hat{H}_{\mathrm{DC}} \Psi_I = E_I \Psi_I, \tag{9}$$

with Ψ_I and E_I being the Ith eigenfunction and eigenvalue of the Dirac-Coulomb Hamiltonian being given by

$$\hat{H}_{\mathrm{DC}} = \sum_{i}^{N_{\mathrm{elec}}} \Bigg[c\boldsymbol{\gamma}^0 \vec{\boldsymbol{\gamma}} \cdot \hat{\vec{p}}_i + (\boldsymbol{\gamma}^0 - \mathbf{1}) m_{\mathrm{e}} c^2 + V_{\mathrm{nuc}}(\vec{r}_i) + \frac{1}{2} \sum_{j \neq i}^{N_{\mathrm{elec}}} k_{\mathrm{es}} \frac{e^2}{|\vec{r}_i - \vec{r}_j|} \Bigg], \tag{10}$$

where we shifted the energy levels by $-m_{\mathrm{e}}c^2$ to bring the upper part of the spectrum into correspondence with the nonrelativistic limit of the energy levels. Here e is the elementary electric charge, and k_{es} is in SI units $\frac{1}{4\pi\epsilon_0}$ with ϵ_0 being the electric constant and V_{nuc} being the potential the nuclei in the molecule produce.

In the Dirac-Hartree-Fock-Coulomb (DHFC) approach, the multielectron states Ψ_I are approximated by a Slater determinant build from an orthonormal set of single-electron bi-spinors ψ_i with orbital energy ϵ_i. From the lower equation of the resulting single-electron Dirac equations expressions for the lower components χ_i of the Dirac bispinors

$$\psi_i(\vec{r}) = \begin{pmatrix} \varphi_i(\vec{r}) \\ \chi_i(\vec{r}) \end{pmatrix} \tag{11}$$

can be found via

$$\chi_i(\vec{r}) = c(2m_{\mathrm{e}}c^2 - \hat{V} + \varepsilon_i)^{-1} \vec{\boldsymbol{\sigma}} \cdot \hat{\vec{p}}\, \varphi_i(\vec{r}), \tag{12}$$

where we have omitted all multielectron effects for the sake of simplifying the discussion below.

For the remaining part of this section, we will use atomic units, in which $\hbar$, $|e|$, and m_{e} have the numerical value of 1. Then, the term in parentheses in Eq. (12) can be expanded in orders of the fine structure constant $\alpha = c^{-1}$ as

$$c(2c^2 - \hat{V} + \varepsilon_i)^{-1} = \frac{\alpha}{2} \sum_{k=0}^{\infty} \left[\frac{\alpha}{2}(\hat{V} - \varepsilon_i) \right]^k. \tag{13}$$

Truncation after first order yields the Pauli approximation

$$\chi_i(\vec{r}) = \left[\frac{\alpha}{2} + \frac{\alpha^3}{4}(\hat{V} - \varepsilon_i) \right] \vec{\boldsymbol{\sigma}} \cdot \hat{\vec{p}}\, \varphi_i(\vec{r}). \tag{14}$$

In a molecule, the expectation value of $\boldsymbol{\gamma}^5$ for a single Slater determinant is determined by a summation over contributions from all occupied molecular orbitals i:

$$\langle \psi_i \,|\, \boldsymbol{\gamma}^5 \,|\, \psi_i \rangle = \langle \varphi_i \,|\, \chi_i \rangle + \langle \chi_i \,|\, \varphi_i \rangle. \tag{15}$$

Insertion of the first term of the expansion Eq. (14) into Eq. (15) gives the first-order contribution to $\boldsymbol{\gamma}^5$:

$$\langle \psi_i \,|\, \boldsymbol{\gamma}^5 \,|\, \psi_i \rangle \approx \alpha \langle \varphi_i \,|\, \vec{\boldsymbol{\sigma}} \cdot \hat{\vec{p}} \,|\, \varphi_i \rangle. \tag{16}$$

This obviously vanishes if the overall electron density of the molecule is nonhelical, but can, in the static case and when remaining in first order with respect to $\mathcal{P}$-odd operators, only be nonzero for a chiral molecule, in which the electron density can have nonvanishing helicity.

In order to determine scaling laws with respect to the nuclear charge number Z and the fine-structure constant α, Eq. (15) itself is not immediately useful. This is why we follow Ref. [27] and write the operator $\boldsymbol{\gamma}^5$ for electron i as a commutator:

$$\boldsymbol{\gamma}_i^5 = \frac{\imath}{c}[\hat{H}_{\mathrm{DC}}, \vec{\boldsymbol{\Sigma}}_i \cdot \vec{r}_i]_- + 2\begin{pmatrix} \mathbf{0} & \hat{\mathbf{k}}_i \\ \hat{\mathbf{k}}_i & \mathbf{0} \end{pmatrix}, \tag{17}$$

$$\hat{\mathbf{k}}_i = -(\mathbf{1}_i + \vec{\boldsymbol{\sigma}}_i \cdot \hat{\vec{l}}_i)\,, \quad \vec{\boldsymbol{\Sigma}}_i = \begin{pmatrix} \vec{\boldsymbol{\sigma}}_i & \mathbf{0} \\ \mathbf{0} & \vec{\boldsymbol{\sigma}}_i \end{pmatrix}. \tag{18}$$

Eigenvalues of the operator $\hat{\mathbf{K}} = \sum_i \hat{\mathbf{k}}_i$ in atomic systems correspond to the relativistic quantum numbers $\varkappa = (\ell - j)(2j + 1)$, where ℓ and j are the orbital and total angular momentum quantum numbers, respectively.

As long as we are interested in expectation values of the operator $\boldsymbol{\gamma}^5$ on the molecular DHFC orbitals ψ_i, the commutator part in Eq. (17) turns to zero. DHFC molecular orbital matrix elements of the second term in Eq. (17) have the form

$$\langle \psi_i \,|\, \boldsymbol{\gamma}^5 \,|\, \psi_i \rangle = 2\langle \varphi_i \,|\, \hat{\mathbf{k}} \,|\, \chi_i \rangle + 2\langle \chi_i \,|\, \hat{\mathbf{k}} \,|\, \varphi_i \rangle. \tag{19}$$

The nonrelativistic limit of $\langle \boldsymbol{\gamma}^5 \rangle$ vanishes as can be shown by insertion of the first term of the expansion Eq. (14) into Eq. (19):

$$\langle \psi_i \,|\, \boldsymbol{\gamma}^5 \,|\, \psi_i \rangle \approx \alpha \langle \varphi_i \,|\, \{\hat{\mathbf{k}}, \vec{\boldsymbol{\sigma}} \cdot \hat{\vec{p}}\}_+ \,|\, \varphi_i \rangle = 0, \tag{20}$$

where we use the fact that operator $\hat{\mathbf{k}}$ anticommutes with $\vec{\boldsymbol{\sigma}} \cdot \hat{\vec{p}}$:

$$\{\hat{\mathbf{k}}, \vec{\boldsymbol{\sigma}} \cdot \hat{\vec{p}}\}_+ = 0. \tag{21}$$

The terms of order α^3 give

$$\langle \psi_i \,|\, \boldsymbol{\gamma}^5 \,|\, \psi_i \rangle \approx \frac{\alpha^3}{2} \langle \varphi_i \,|\, (\vec{\boldsymbol{\sigma}} \cdot \hat{\vec{p}})\hat{V}\hat{\mathbf{k}} + \hat{\mathbf{k}}\hat{V}(\vec{\boldsymbol{\sigma}} \cdot \hat{\vec{p}}) \,|\, \varphi_i \rangle, \tag{22}$$

where the terms containing orbital energies ε_i reduce to the anticommutator Eq. (21). Equation (22) can be rewritten as

$$\begin{aligned}\langle\psi_i\,|\,\boldsymbol{\gamma}^5\,|\,\psi_i\rangle &\approx \frac{\alpha^3}{2}\langle\varphi_i\,|\,[\vec{\boldsymbol{\sigma}}\cdot\hat{\vec{p}},\hat{V}(\vec{r})]_-\hat{\mathbf{k}}+\hat{V}(\vec{r})\{\hat{\mathbf{k}},\vec{\boldsymbol{\sigma}}\cdot\hat{\vec{p}}\}_+\\ &\quad+[\hat{\mathbf{k}},\hat{V}(\vec{r})]_-\vec{\boldsymbol{\sigma}}\cdot\hat{\vec{p}}\,|\,\varphi_i\rangle\\ &=\frac{\alpha^3}{2}\langle\varphi_i\,|\,[\vec{\boldsymbol{\sigma}}\cdot\hat{\vec{p}},\hat{V}(\vec{r})]_-\hat{\mathbf{k}}\\ &\quad+[\hat{\mathbf{k}},\hat{V}(\vec{r})]_-\vec{\boldsymbol{\sigma}}\cdot\hat{\vec{p}}\,|\,\varphi_i\rangle,\end{aligned}\tag{23}$$

where we once again used Eq. (21). In general, the molecular potential energy operator $\hat{V}$ does not commute with both operators $\hat{\mathbf{k}}$ and $(\vec{\boldsymbol{\sigma}}\cdot\hat{\vec{p}})$. However, its spherically symmetric part $\hat{V}_{\mathrm{s}}(|\vec{r}|)$ commutes with the operator $\hat{\mathbf{k}}$. Therefore, for the spherically symmetric potential the last term in Eq. (23) turns to zero. Let us separate the contribution of $\hat{V}_{\mathrm{s}}(|\vec{r}|)$:

$$\langle\psi_i\,|\,\boldsymbol{\gamma}^5\,|\,\psi_i\rangle=\langle\psi_i\,|\,\boldsymbol{\gamma}^5\,|\,\psi_i\rangle_{\mathrm{s}}+\langle\psi_i\,|\,\boldsymbol{\gamma}^5\,|\,\psi_i\rangle_{\mathrm{a}},\tag{24}$$

$$\langle\psi_i\,|\,\boldsymbol{\gamma}^5\,|\,\psi_i\rangle_{\mathrm{s}}=\frac{\alpha^3}{2}\langle\varphi_i\,|\,-\imath(\vec{\boldsymbol{\sigma}}\cdot\vec{r})\frac{\hat{V}_{\mathrm{s}}'(|\vec{r}|)}{|\vec{r}|}\hat{\mathbf{k}}\,|\,\varphi_i\rangle\tag{25}$$

and consider the term Eq. (25) in more detail. Note that $\hat{V}_{\mathrm{s}}'(|\vec{r}|)/|\vec{r}|$ commutes with both operators $\vec{\boldsymbol{\sigma}}\cdot\vec{r}$ and $\hat{\mathbf{k}}$. By analogy with Eq. (21), we can assume that $\{\vec{\boldsymbol{\sigma}}\cdot\vec{r},\hat{\mathbf{k}}\}_+=0$. Thus, we can write

$$\imath(\vec{\boldsymbol{\sigma}}\cdot\vec{r})\hat{\mathbf{k}}=\frac{\imath}{2}[\vec{\boldsymbol{\sigma}}\cdot\vec{r},\hat{\mathbf{k}}]_-,\tag{26}$$

which proves that the operator in Eq. (25) is Hermitian, and allows us to rewrite this expression as

$$\langle\psi_i\,|\,\boldsymbol{\gamma}^5\,|\,\psi_i\rangle_{\mathrm{s}}=\frac{\alpha^3}{4}\langle\varphi_i\,|\,\vec{\boldsymbol{\sigma}}\cdot\vec{v}_{\mathcal{T},\mathrm{s}}\,|\,\varphi_i\rangle,\tag{27}$$

$$\vec{v}_{\mathcal{T},\mathrm{s}}=\frac{\hat{V}_{\mathrm{s}}'(|\vec{r}|)}{|\vec{r}|}(|\vec{r}|^2\hat{\vec{p}}-\vec{r}(\hat{\vec{p}}\cdot\vec{r})).\tag{28}$$

We see that expectation value Eq. (27) has the form of a scalar product of the spin with an electronic orbital $\mathcal{T}$-odd vector $\vec{v}_{\mathcal{T},\mathrm{s}}$. Molecular matrix elements of $\vec{\boldsymbol{\sigma}}\cdot\vec{v}_{\mathcal{T}}$ turn to zero in the nonrelativistic approximation for two reasons: (i) For a singlet state, an expectation value of the spin is zero, and (ii) matrix elements of orbital $\mathcal{T}$-odd vectors are imaginary, so their expectation values are zero. In order to get a nonzero expectation value of such operators, one needs to include spin-orbit interactions $\hat{H}_{\mathrm{so}}$, which mix singlet and triplet molecular states and have imaginary matrix elements. Therefore, the energy shift $\delta E_{\gamma^5,\mathrm{s}}$ of the molecular (ground) singlet state due to the interaction $\vec{\boldsymbol{\sigma}}\cdot\vec{v}_{\mathcal{T},\mathrm{s}}$ appears in double perturbation theory as

$$\delta E_{\gamma^5,\mathrm{s}}\sim\frac{\alpha^3}{2}\frac{2\mathrm{Re}\{\langle\Psi_{\mathrm{s}}\,|\,\vec{\boldsymbol{\sigma}}\cdot\vec{v}_{\mathcal{T},\mathrm{s}}\,|\,\Psi_{\mathrm{t}}\rangle\langle\Psi_{\mathrm{t}}\,|\,\hat{H}_{\mathrm{so}}\,|\,\Psi_{\mathrm{s}}\rangle\}}{E_{\mathrm{s}}-E_{\mathrm{t}}},\tag{29}$$

where E_{s}, E_{t} and Ψ_{s}, Ψ_{t} are the nonrelativistic singlet and triplet energies and wave functions, respectively.

Equation (29) allows us to estimate the scaling law for $\delta E_{\gamma^5,\mathrm{s}}$ with the nuclear charge Z and the fine structure constant α. The matrix element of the spin-orbit interaction $\langle\psi_{\mathrm{t}}\,|\,\hat{H}_{\mathrm{so}}\,|\,\psi_{\mathrm{s}}\rangle$ scales as α^2Z^2. The Z scaling of the matrix element of the operator $\vec{v}_{\mathcal{T},\mathrm{s}}$ depends on the distances where the integral is accumulated. Taking into account that this operator appears in third order in α, we can assume that the integral is accumulated at short distances near the nucleus, where relativistic corrections are larger. At such distances, the potential of the nucleus is practically unscreened, $\hat{V}_{\mathrm{s}}\sim Z/r$. Furthermore, at these distances the electron moves Z times faster, so $\hat{\vec{p}}\sim Z$. Therefore, we can assume that $\int v_{\mathcal{T},\mathrm{s}}d^3r\sim Z^2$. Then the overall scaling is

$$\delta E_{\gamma^5,\mathrm{s}}\sim\alpha^5Z^4\,.\tag{30}$$

The last expression does not take into account "the single center theorem" [54,55], which implies that electron helicity in molecules is suppressed in the vicinity of a single heavy main group nucleus and one has to take two matrix elements of expression Eq. (29) at two different heavy main group centers. Therefore, the final scaling should be in this case

$$\delta E_{\gamma^5,\mathrm{s}}\sim\alpha^5Z_A^2Z_B^2\,,\tag{31}$$

where A and B are typically taken as the two heaviest atoms in the molecule.

Now let us analyze the second term in Eq. (24). In this case, both terms from Eq. (23) can contribute. For the first term, we can use the same arguments as above, but the asymmetric part of the molecular potential at short distances is much weaker, so this term will add small corrections to Eq. (31). Thus, we will focus on the second term, which was zero for the symmetric potential.

We assume again that the matrix element is accumulated at short distances, where the molecular potential can be expanded in spherical harmonics [56]. The second term of this expansion can be written as $(\vec{a}\cdot\vec{r})\hat{V}_{\mathrm{a}}(|\vec{r}|)$, where $\vec{a}$ is some constant polar vector. In this approximation, we get

$$[\hat{\mathbf{k}},\hat{V}(|\vec{r}|)]_-=-\imath[\vec{\boldsymbol{\sigma}}\cdot(\vec{r}\times\vec{a})]\hat{V}_{\mathrm{a}}(|\vec{r}|).\tag{32}$$

Substituting this into the second term in Eq. (23), we find that

$$\langle\psi_i\,|\,\boldsymbol{\gamma}^5\,|\,\psi_i\rangle_{\mathrm{a}}\approx\frac{\alpha^3}{2}\langle\varphi_i\,|\,-\imath(\vec{\boldsymbol{\sigma}}\cdot\vec{r}\times\vec{a})\hat{V}_{\mathrm{a}}(|\vec{r}|)(\vec{\boldsymbol{\sigma}}\cdot\hat{\vec{p}})\,|\,\varphi_i\rangle.\tag{33}$$

Simplifying this further and neglecting the term which is similar to Eq. (28), we get

$$\langle\psi_i\,|\,\boldsymbol{\gamma}^5\,|\,\psi_i\rangle_{\mathrm{a}}\approx\frac{\alpha^3}{2}\langle\varphi_i\,|\,\vec{a}\cdot\vec{v}_{\mathrm{a}}\,|\,\varphi_i\rangle,\tag{34}$$

$$\vec{v}_{\mathrm{a}}=2\hat{V}_{\mathrm{a}}(|\vec{r}|)\,\vec{r}\times\vec{\nabla}\,.\tag{35}$$

The orbital pseudovector $\vec{v}_{\mathrm{a}}$ is $\mathcal{T}$ even. The expected scaling with α is given by Eq. (34). Scaling with Z for operators Eqs. (28) and (35) should be similar, so we assume

$$\delta E_{\gamma^5,\mathrm{a}}\sim\alpha^3Z^2\,.\tag{36}$$

Combining the two terms in Eq. (24) together suggests an estimate for a molecule with two heavy main group atoms A and B:

$$\delta E_{\gamma^5}\approx c_1\alpha^5Z_A^2Z_B^2+c_2\alpha^3Z_A^2+c_3\alpha^3Z_B^2\,.\tag{37}$$

The first term is formed on both heavy centers, while the other two terms are formed independently in the vicinity of each heavy nucleus. The chiral structure of the molecule is weakly felt locally [54,56], so we can expect that $|c_{2,3}|\ll|c_1|$.

TABLE I. Molecular structure parameters for compounds of type H_2X_2 and H_2XO with X = O, S, Se, Te, or Po employed in all calculations. Parameters for H_2X_2 were taken from Refs. [58,65]. O–X bond length determined by full structure optimization of eH_2XO compounds at the level of ZORA-cGHF.

X	$r(X-X)$ (Å)	$r(X-\mathrm{O})$ (Å)	$r(X-\mathrm{H})$ (Å)	$\sphericalangle(X-X-\mathrm{H})$ (deg)
O	1.490	1.490	0.970	100
S	2.055	1.627	1.352	92
Se	2.480	1.768	1.450	92
Te	2.840	1.933	1.640	92
Po	2.910	2.057	1.740	92

TABLE II. Electronic expectation value of $\boldsymbol{\gamma}^5$ for (P) enantiomers of compounds of type H_2XO and H_2X_2 at a dihedral angle of 45° calculated at the level of ZORA-cGHF.

	$\langle \boldsymbol{\gamma}_5 \rangle$	
Z_X	H_2XO	H_2X_2
8	7.02×10^{-9}	7.02×10^{-9}
16	1.81×10^{-8}	7.23×10^{-8}
34	9.66×10^{-8}	2.87×10^{-6}
52	2.67×10^{-7}	1.95×10^{-5}
84	8.69×10^{-7}	2.11×10^{-4}

In the following, we discuss the implications in molecular systems of the equation derived above for $\langle \boldsymbol{\gamma}^5 \rangle$ and compare to results from numerical computations. Hereby, we focus on scaling with respect to the nuclear charge number and the fine structure constant. Furthermore, we compare to energy shifts due to nuclear spin-independent electroweak neutral-current interactions.

III. COMPUTATIONAL DETAILS

Quasirelativistic two-component calculations of H_2X_2 and H_2XO with X = O, S, Se, Te, Po, and CHBrClF are performed within the zeroth-order regular approximation (ZORA) at the level of complex generalized Hartree-Fock (cGHF) or Kohn-Sham (cGKS) with a modified version [57–63] of the quantum chemistry program package TURBOMOLE [64].

For calculations of H_2X_2 and H_2XO compounds, a basis set of 25 s, 25 p, 14 d, and 11 f uncontracted Gaussian functions with the exponential coefficients α_i composed as an even-tempered series by $\alpha_i = a \cdot b^{N-i}$; $i = 1, \ldots, N$ with $a = 0.02 a_0^{-2}$, $b = (5/2 \times 10^{10})^{1/25} \approx 2.606$ and $N = 26$ was used for X = O, S, Se, Te, and Po. The largest exponent coefficients of the s, p, d, and f subsets are $5 \times 10^8\, a_0^{-2}$, $1.91890027 \times 10^8\, a_0^{-2}$, $13300.758\, a_0^{-2}$, and $751.8368350\, a_0^{-2}$, respectively. A similar but slightly smaller basis set (three f functions less) has proven successful in calculations of $\mathcal{P}$-violating energy shifts in H_2Po_2 [58,65]. The H atom was represented with the s,p-subset of a decontracted correlation-consistent basis of quadruple-ζ quality [66].

Structure parameters of H_2X_2 were chosen as in Refs. [58,65]. For H_2XO compounds, the equilibrium bond length of the O–X bond, for X = S, Se, Te, or Po, was obtained by full structure optimization at the level of ZORA-cGHF. As convergence criteria, an energy change of less than $10^{-5}\, E_\mathrm{h}$ was used. Bond angles H–O–X and bond distances H–O of H_2XO were assumed to be equal to H_2O_2 and bond angles H–X–O and distances H–X were assumed to be equal to H_2X_2. Employed structure parameters are summarized in Table I.

Structure parameters, harmonic vibrational wave numbers, and normal coordinates, of CHBrClF, as well as electronic densities and vibrational wave functions along the C–F stretching mode, were employed as described in Ref. [67]. Electronic densities along other normal coordinates were calculated on the level of ZORA-cGHF and ZORA-cGKS with the same basis set employed in Ref. [67]. Properties were calculated on the levels of ZORA-cGHF and ZORA-cGKS. Used density functionals are the local density approximation (LDA) [68–70] and the Lee, Yang, and Parr correlation functional (LYP) [71] with a generalized gradient exchange functional by Becke (BLYP) [72] or the hybrid Becke three-parameter exchange functional (B3LYP) [69,73–75].

The ZORA-model potential $\tilde{V}(\vec{r})$ as proposed by van Wüllen [76] was employed with additional damping [77].

For calculations of two-component wave functions and properties, a finite nucleus was used, described by a normalized spherical Gaussian nuclear density distribution $\rho_{\mathrm{nuc},A}(\vec{r}) = \frac{\zeta_A^{3/2}}{\pi^{3/2}} e^{-\zeta_A |\vec{r}-\vec{r}_A|^2}$, where $\zeta_A = \frac{3}{2 r^2_{\mathrm{nuc},A}}$ and the root mean square radius $r_{\mathrm{nuc},A}$ of nucleus A was used as suggested by Visscher and Dyall [78]. The mass numbers A were chosen to correspond to the isotopes ^{1}H, ^{12}C, ^{16}O, ^{19}F, ^{32}S, ^{35}Cl, ^{79}Br, ^{80}Se, ^{130}Te, and ^{209}Po. The weak nuclear charges $Q_{\mathrm{W},A}$ of the various isotopes with charge number Z_A and neutron number N_A were included as $Q_{\mathrm{W},A} \approx (1 - 4\sin^2\theta_\mathrm{W})Z_A - N_A$, where we have used $\sin^2\theta_\mathrm{W} = 0.2319$ as the numerical value of the Weinberg parameter.

All relativistic expectation values of $\boldsymbol{\gamma}^5$ and $\hat{H}_\mathrm{ew}$ were calculated with our ZORA property toolbox approach described in Ref. [63].

IV. RESULTS

A. Scaling laws for $\langle \boldsymbol{\gamma}^5 \rangle$ in molecules

In order to confirm results of Sec. II B we performed quasirelativistic numerical calculations at the level of ZORA of (P) enantiomers of H_2X_2 compounds with a dihedral angle of 45°, varying X = O, S, Se, Te, and Po. These compounds are established as a common test system for electroweak $\mathcal{P}$ violation and its scaling behavior with respect to nuclear charge [58–60,65,79–81]. In the above scaling law, a factor of $\alpha^2 Z_B^2$ emerges from spin-orbit coupling. This factor is in good approximation equal to α^2 in main group element containing molecules with only one heavy center (see, e.g., Refs. [54]). Therefore, for a variation of one heavy X atom while holding the other one fixed as oxygen atom (H_2XO), we would expect roughly a scaling of $\sim\alpha^3 Z_A^2$ [corresponding to the second term in Eq. (37)] as the spin-orbit coupling contribution [corresponding to the first term in Eq. (37)] is suppressed by a factor of α^2.

The numerical results are summarized in Tables II and III. Figure 1 shows a double logarithmic plot and a linear fit for

TABLE III. Electronic expectation value of $\boldsymbol{\gamma}^5$ for (P) enantiomers of H_2PoO and H_2Po_2 at a dihedral angle of 45° calculated at the level of ZORA-cGHF for different values of the fine structure constant α including α_0 which is $\frac{1}{c}$ in atomic units.

	$\langle\boldsymbol{\gamma}_5\rangle$	
α	H_2PoO	H_2Po_2
$\frac{1}{90}$	3.20×10^{-7}	1.38×10^{-3}
α_0	8.69×10^{-7}	2.11×10^{-4}
$\frac{1}{300}$	3.42×10^{-8}	2.10×10^{-6}
$\frac{1}{400}$	1.23×10^{-9}	4.60×10^{-7}
$\frac{1}{1000}$	6.65×10^{-10}	4.33×10^{-9}

the determination of the Z-scaling law in ZORA-cGHF calculations. From numerical calculations of H_2X_2 compounds, we find a Z scaling with $Z^{4.4}$, which agrees well with the analytical prediction. Furthermore, for H_2XO compounds, we find a scaling of $Z^{2.1}$, which is in perfect agreement with the expectations above and shows the missing spin-orbit coupling contribution as the nuclear charge of oxygen is close to 1.

In order to test the predicted α dependence, the speed of light was varied in the quasirelativistic calculations of wave functions and properties for H_2PoO and H_2Po_2. The results (see Figure 2) display the expected scaling of $\alpha^{5.4} \approx \alpha^5$ for H_2Po_2 and a scaling of $\alpha^{3.6}$ for H_2PoO, showing the weak influence of spin-orbit coupling in compounds with only one heavy nucleus. The results are in perfect agreement with the analytical analysis.

B. Comparison to electroweak electron-nucleon interactions

Similar considerations, as detailed in the previous section, are known to hold also for parity-nonconserving nuclear spin-independent electroweak interactions described by Hamiltonian Eq. (8) in chiral molecules. The main difference of this Hamiltonian to the ones discussed in the theory section is that $\hat{H}_{\mathrm{ew}}$ evaluates the expectation value of $\boldsymbol{\gamma}^5$ at positions inside the nuclei only. To further compare $\hat{H}_{\mathrm{ew}}$ with $\boldsymbol{\gamma}^5$, we evaluated the dependence of the expectation value of both operators on the dihedral angle in H_2X_2 for X = O and Po, and found similar behavior (see Fig. 3, and for the explicit data see the Supplemental Material [82]). It shall be noted that

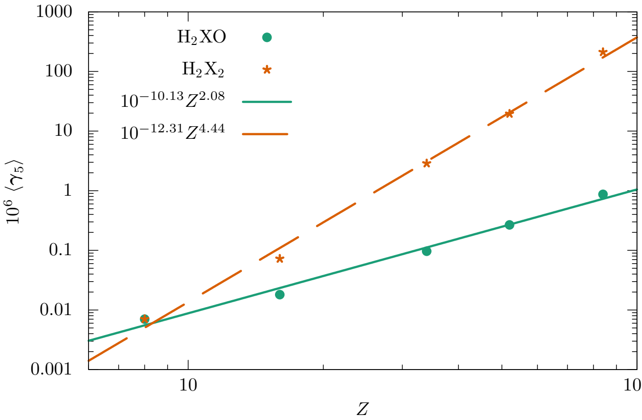

FIG. 1. Dependence of the expectation value of $\boldsymbol{\gamma}^5$ on the nuclear charge Z for the (P) enantiomers of H_2X_2 and H_2XO with X = O, S, Se, Te, or Po at an dihedral angle of 45° calculated at the ZORA-cGHF level.

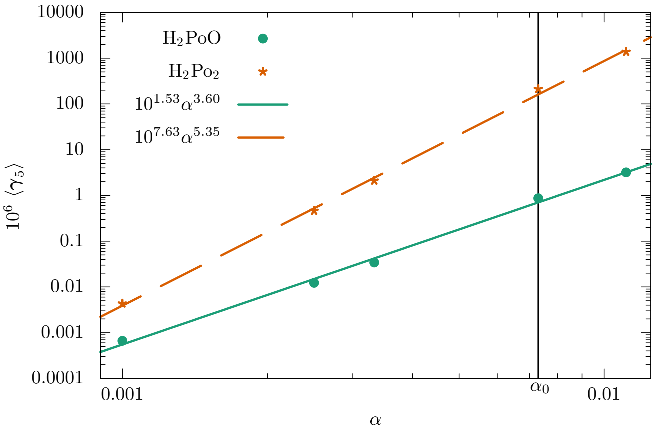

FIG. 2. Dependence of the expectation value of $\boldsymbol{\gamma}^5$ on the fine structure constant α for the (P) enantiomers of H_2Po_2 and H_2PoO at an dihedral angle of 45° calculated at the ZORA-cGHF level.

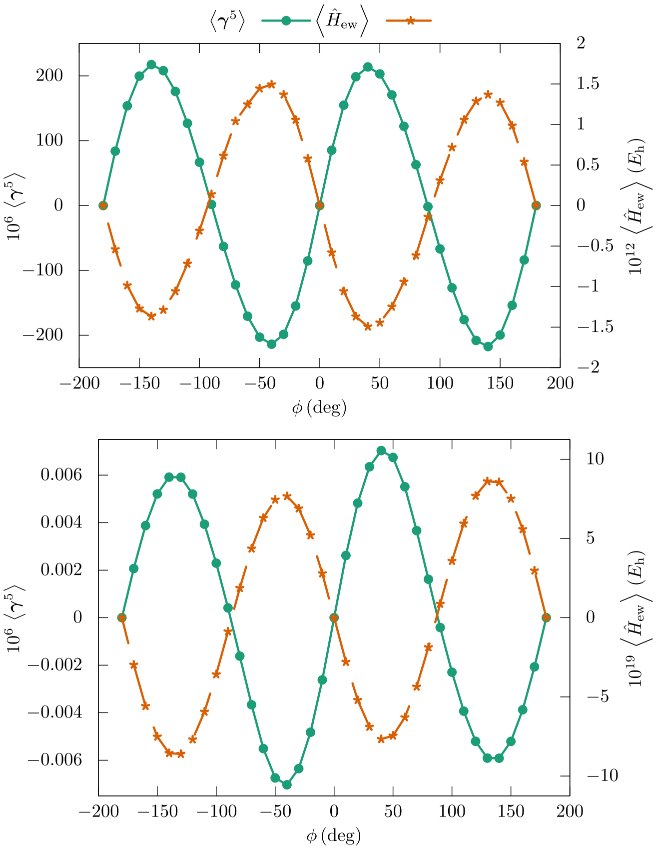

FIG. 3. Dependence of the expectation value of $\boldsymbol{\gamma}^5$ in comparison to the expectation value of $\hat{H}_{\mathrm{ew}}$ on the dihedral angle ϕ in H_2Po_2 (top) and H_2O_2 (bottom) calculated at the ZORA-cGHF level. The results on $\hat{H}_{\mathrm{ew}}$ slightly differ from those of Ref. [58] due to the use of a different basis set. Straight lines connecting the computed points are drawn to guide the eye.

the sign of $\hat{H}_{\text{ew}}$ is inverted in comparison to $\boldsymbol{\gamma}^5$ as $\hat{H}_{\text{ew}}$ contains in addition the weak charge for which $Q_{\text{W}} \approx -N < 0$.

In a recent work [83], similar calculations on $\boldsymbol{\gamma}^5$ in H_2X_2 compounds were performed and similar results were obtained. However, unfortunately, in Ref. [83] insufficient basis sets for oxygen were employed, resulting in qualitatively wrong results for the dihedral angle dependence in H_2O_2.

The similar dependence on the molecular structure together with the steep scaling with nuclear charge indicates that contributions at the nuclear centers dominate also the expectation value of $\boldsymbol{\gamma}^5$ and thus implies that molecular experiments that aim to test $\mathcal{P}$ violation due to weak interactions can also be used for searches of $\mathcal{P}$-odd cosmic field interactions with a comparable sensitivity. This aspect will be discussed in the following in detail.

C. Limits on cosmic fields from experiments with chiral molecules

1. Test system and choice of methods

The expected sensitivity of experiments with chiral molecules to $\mathcal{P}$-odd cosmic field interactions characterized by b_0^{e} is estimated from an experiment with CHBrClF performed by Daussy *et al.* [46], in which a hyperfine component of the $40_{7,34} \leftarrow 40_{8,33}$ transition ($J'_{K'_a,K'_c} \leftarrow J''_{K''_a,K''_c}$) of the C–F stretching fundamental in enantiomerically enriched samples of the mirror images *R*-CHBrClF and *S*-CHBrClF was studied.

Our interest is in a possible splitting of the vibrational resonance frequency between enantiomers that is caused by cosmic fields interacting through $\langle \boldsymbol{\gamma}^5 \rangle$. For this purpose, frequency shifts in the vibrational spectrum due to electronic interactions via $\boldsymbol{\gamma}^5$ have to be evaluated. This test system, CHBrClF, was excessively studied by theory [67,84–91] and experiment [44–46,92,93] and is supposed to be reasonably well understood with respect to electroweak $\mathcal{P}$ violation.

However, the influence from nonseparable anharmonic effects (multimode effects) on electroweak $\mathcal{P}$ violation in CHBrClF is largely unexplored. Quack and Stohner studied the deuterated isotopomer CDBrClF [94] with respect to multimode contributions in a four-dimensional, anharmonically treated subspace involving the C–F stretch, C–D stretch, and the two C–D bending modes to find an increase of the $\mathcal{P}$-odd frequency splitting in the C–F stretch fundamental ν_4 by almost a factor of 2—depending on the specific model, they obtained up to 75% relative deviation with respect to the separable anharmonic adiabatic approximation. Although not directly comparable due to the different isotope, this at least suggests that pronounced multimode effects can also exist for $\langle \boldsymbol{\gamma}^5 \rangle$.

We have reported major findings and implications for future experiments in a separate paper [1], but provide herein more details on the computational challenges and subsequent analysis.

We estimate the influence of multimode effects within a perturbative treatment by calculation of derivatives of the property of interest with respect to all normal coordinates. One-dimensional and two-dimensional vibrational corrections to a property O for a single dimensionless reduced normal coordinate q_r are in leading order given by [95]

$$O_{q_r}^{\text{1D}} \approx \frac{1}{2}\left(v_r + \frac{1}{2}\right)\left(\frac{\partial^2 O_0}{\partial q_r^2} - \frac{\phi_{rrr}}{\tilde{\nu}_r}\frac{\partial O_0}{\partial q_r}\right), \tag{38}$$

$$O_{q_r}^{\text{2D}} \approx -\frac{1}{2}\left(v_r + \frac{1}{2}\right)\sum_{s\neq r}\frac{\phi_{rrs}}{\tilde{\nu}_s}\frac{\partial O_0}{\partial q_s}, \tag{39}$$

where ϕ_{rst} are the cubic force constants and $\tilde{\nu}_r$ are the harmonic vibrational wave numbers.

Properties are evaluated along the dimensionless reduced normal coordinate q_r and fitted to a polynomial of degree 4:

$$\langle \psi_{\text{e}} \,|\, \hat{H}_{\text{ew}} \,|\, \psi_{\text{e}} \rangle_r \approx \sum_{k=0}^{4} c_{\text{ew},r,k}\, q_r^k, \tag{40}$$

$$\langle \psi_{\text{e}} \,|\, \boldsymbol{\gamma}^5 \,|\, \psi_{\text{e}} \rangle_r \approx \sum_{k=0}^{4} c_{\gamma^5,r,k}\, q_i^k. \tag{41}$$

In Fig. 4, the dependence of $\langle \boldsymbol{\gamma}^5 \rangle$ and $\langle \hat{H}_{\text{ew}} \rangle$ on the normal coordinates for the different methods in the region $q_r = -3, \ldots, 3$ (for the explicit data, see the Supplemental Material [82]). Within this region, the probability density of the first two vibrational states in the mode q_4 is sufficiently decayed (see Fig. 1 of Ref. [67]), as can also be expected by considering classical turning points of a harmonic approximation to the parity-conserving potential, which are located at $|q_4| = 1$ for the ground vibrational state of a harmonic oscillator and at $|q_4| = \sqrt{3}$ in the first vibrationally excited state. The resulting fit parameters $c_{\gamma^5,r,k}$ alongside the explicit values for the one-dimensional cuts through the hypersurface for all normal coordinates q_r are reported in the Supplemental Material [82].

The derivatives of the properties with respect to the normal coordinate q_r are given by

$$\frac{\partial \langle \psi_{\text{e}} \,|\, \boldsymbol{\gamma}^5 \,|\, \psi_{\text{e}} \rangle_r}{\partial q_r} = c_{\gamma^5,r,1}, \tag{42}$$

$$\frac{\partial^2 \langle \psi_{\text{e}} \,|\, \boldsymbol{\gamma}^5 \,|\, \psi_{\text{e}} \rangle_r}{\partial q_r^2} = 2c_{\gamma^5,r,2}, \tag{43}$$

and analogously for $\hat{H}_{\text{ew}}$. Resulting first and second derivatives from the fit in Fig. 4 are listed in Tables V and VI. From these, we see that the C–F stretching mode has a weak influence on $\langle \boldsymbol{\gamma}^5 \rangle$ in comparison to the other modes and, thus, is not an optimal choice for an experiment. In particular, along the deformation normal coordinates q_9 (Br–Cl), q_8 (Br–F), q_3 (H), and q_2 (H), the first derivatives of $\langle \boldsymbol{\gamma}^5 \rangle$ are considerably larger in magnitude than for q_4. The second derivatives with respect to the C-F stretching coordinate are smaller in absolute value than those first derivatives mentioned, by about an order of magnitude (see Tables V and VI). We may assume that anharmonic constants can be roughly of the order $\phi_{rrr} \sim O(0.1\tilde{\nu}_r)$ and $\phi_{rrs} \sim O(0.01\tilde{\nu}_s)$ or even larger (see, e.g., Refs. [96,97] for some cubic force constants in CDBrClF). In total, two-dimensional effects on the C–F stretching mode for $\langle \boldsymbol{\gamma}^5 \rangle$ can be on the same order as one-dimensional vibrational effects. Thus, not only is the effect of $\mathcal{P}$-odd interactions on the C-F stretching mode very weak, but also the theoretical description is limited by the need for an excellent description of all modes, which is exceedingly difficult.

TABLE IV. Molecular expectation value of $\boldsymbol{\gamma}^5$ in (S)-CHBrClF for the vibrational ground state and vibrational first excited state along the q_4 normal coordinate (C-F-stretching mode) at the level of ZORA-cGHF (HF) and ZORA-cGKS with LDA, BLYP, and B3LYP functionals within the separable anharmonic adiabatic approximation.

	$\langle\boldsymbol{\gamma}_5\rangle$		
Method	$v = 0,\ (S)$	$v_4 = 1,\ (S)$	$v_4 = 1 \leftarrow v = 0,\ \Delta_{(R,S)}$
HF	-1.89×10^{-9}	-1.71×10^{-9}	3.61×10^{-10}
B3LYP	-8.28×10^{-9}	-7.91×10^{-9}	7.40×10^{-10}
BLYP	-8.27×10^{-9}	-7.82×10^{-9}	9.02×10^{-10}
LDA	-1.21×10^{-8}	-1.15×10^{-8}	1.18×10^{-9}

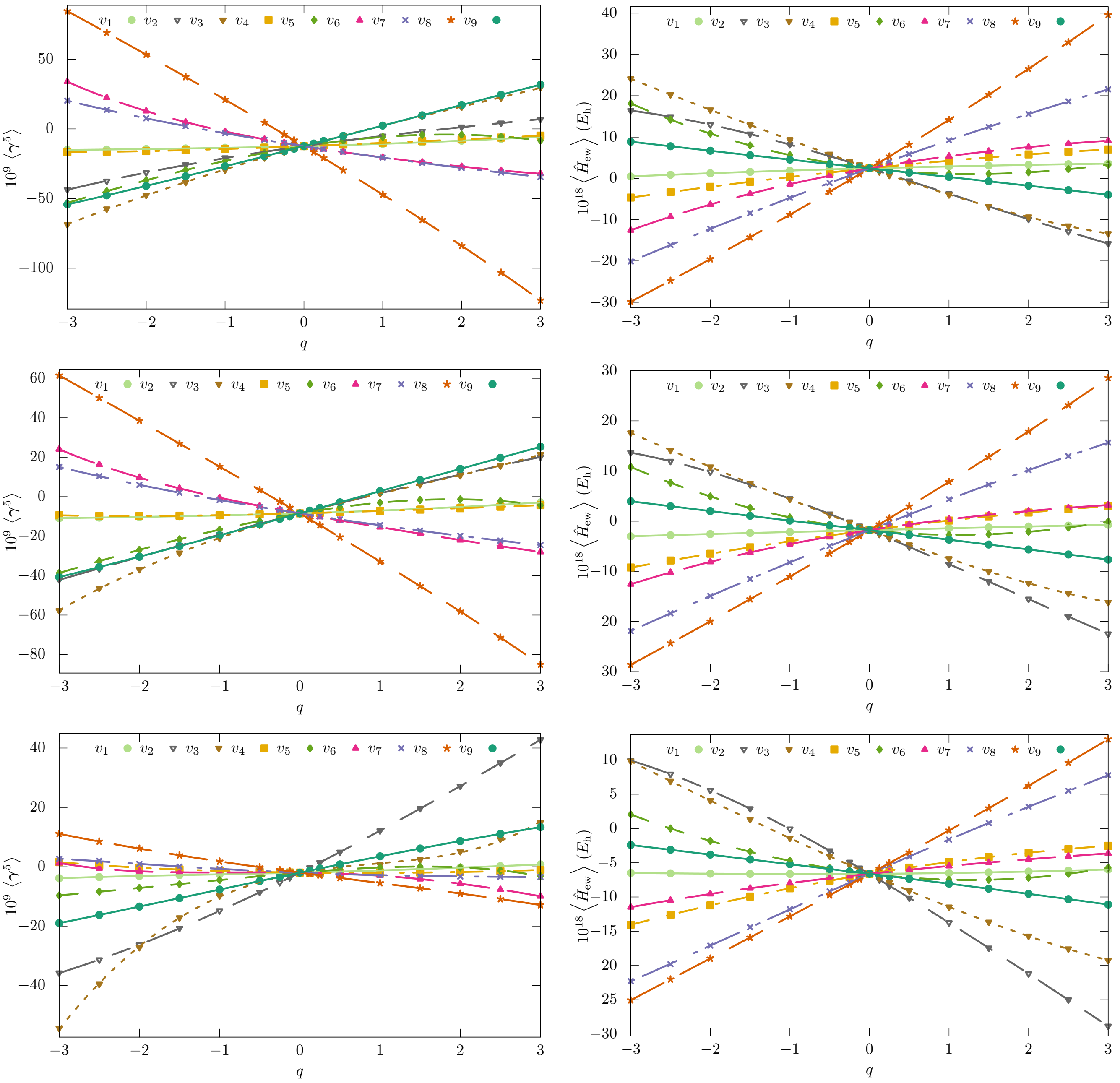

FIG. 4. Dependence of the expectation value of $\boldsymbol{\gamma}^5$ (left) and $\hat{H}_{\mathrm{ew}}$ (right) on the nine normal coordinates in (S)-CHBrClF computed at the ZORA-cGKS and ZORA-cGHF level of theory. Data points are fitted to polynomials of fourth order (lines). (a) $\langle\boldsymbol{\gamma}^5\rangle$, ZORA-cGKS, LDA; (b) $\langle\hat{H}_{\mathrm{ew}}\rangle$, ZORA-cGKS, LDA; (c) figure as of Ref. [1] with values corresponding to $\langle\boldsymbol{\gamma}^5\rangle$, ZORA-cGKS, B3LYP; (d) $\langle\hat{H}_{\mathrm{ew}}\rangle$, ZORA-cGKS, B3LYP; (e) $\langle\boldsymbol{\gamma}^5\rangle$, ZORA-cGHF; and (f) $\langle\hat{H}_{\mathrm{ew}}\rangle$, ZORA-cGHF. Results for $\hat{H}_{\mathrm{ew}}$ in the C–F stretching mode (v_4) are a recalculation of those presented in Ref. [67] and are thus identical to those.

TABLE V. One dimensional first and second derivatives of the molecular expectation value of $\boldsymbol{\gamma}^5$ with respect to the reduced normal coordinate q_r in (S)-CHBrClF at the level of ZORA-cGHF (HF) and ZORA-cGKS with LDA, BLYP, and B3LYP functionals.

	$10^9\,\frac{\partial\langle\boldsymbol{\gamma}^5\rangle}{\partial q_r}$			$10^9\,\frac{\partial^2\langle\boldsymbol{\gamma}^5\rangle}{\partial q_r^2}$		
r	LDA	B3LYP	HF	LDA	B3LYP	HF
9	14.67	11.21	5.63	0.24	0.14	−0.20
8	−34.05	−23.96	−3.61	−1.39	−0.62	0.29
7	−8.71	−6.35	−1.07	1.03	0.74	0.48
6	−9.13	−7.32	−0.39	2.41	0.95	−1.05
5	8.75	6.96	2.26	−4.05	−2.79	−0.73
4	2.21	1.10	−0.31	0.28	0.30	0.46
3	15.65	11.01	4.90	−1.90	−2.39	−4.94
2	7.89	10.47	13.57	−1.37	−0.67	1.22
1	1.42	1.21	0.65	0.46	0.38	0.17

It is important to note that the use of a different vibrational mode [such as Br-F (υ_8) or H (υ_3) deformation] in CHBrClF can result in vibrational frequency splittings that are larger by about an order of magnitude and may reduce error bars considerably. This has to be analyzed in more detail, however, using anharmonic vibrational force fields.

Due to the resulting large error bars for vibrational corrections for the C–F stretching mode, we do not provide a final value for the enhancement of b_0^{e} in the C–F stretching but rather give an order of magnitude estimate.

For this purpose, within the separable anharmonic adiabatic approximation as described in Ref. [85], where we follow for this specific application Ref. [67] closely, the vibrationally averaged expectation value for the C–F stretching mode is evaluated from a series expansion in the vibrational moments $\langle \upsilon \mid q^k \mid \upsilon \rangle$, where υ represents the vibrational quantum number of the υth vibrational state. The vibrational wave functions and corresponding moments were received in Ref. [67] from a discrete variable representation on an equidistant grid. The moments were reported in the supplementary material to Ref. [67] and are reused for calculating interactions of CHBrClF with cosmic fields.

In order to estimate electron correlation effects, for the C–F stretching mode the vibrationally averaged expectation values where evaluated at the DFT and HF level, the former with different flavors of density functionals. The results of these methods are compared in Table IV.

In previous studies on electroweak $\mathcal{P}$-violating vibrational frequency splittings in CHBrClF with density functional approaches [67,90], much reduced variations between the methods were found for the C–F stretching fundamental as can be expected by the nearly parallel curves shown in Fig. 5. In Ref. [67], we have observed a spread of about 20% from the mean value for the four methods used also in the present work. The variation among the various density functionals (B3LYP, BLYP, and LDA) was less than 5%. In Ref. [90], it was found that B3LYP, BLYP, and LDA estimates deviate by 6% or less from the values predicted on the second-order many-body perturbation theory level (MP2), with the latter method giving also absolute values at the equilibrium structure that agree well with the corresponding CCSD(T) estimates. Hartree-Fock-based predictions, in contrast, displayed larger deviations from those of the mentioned density functional calculations. Similar trends are observed in the present work (see Table IV), but with more pronounced variations for the structure dependence of $\langle\boldsymbol{\gamma}^5\rangle$ as compared to $\langle\hat{H}_{\mathrm{ew}}\rangle$: Vibrational splittings vary by about 50% from the mean value of all four methods, with variations among the density functionals being on the order of 25% or less from their mean. Assuming again that the density functionals outperform the

TABLE VI. One-dimensional first and second derivatives of the molecular expectation value of $\hat{H}_{\mathrm{ew}}$ with respect to the reduced normal coordinate q_r in (S)-CHBrClF at the level of ZORA-cGHF (HF) and ZORA-cGKS with LDA, BLYP, and B3LYP functionals.

	$10^{18}\,\frac{\partial\langle\hat{H}_{\mathrm{ew}}\rangle}{\partial q_r}\,(E_{\mathrm{h}})$			$10^{18}\,\frac{\partial^2\langle\hat{H}_{\mathrm{ew}}\rangle}{\partial q_r^2}\,(E_{\mathrm{h}})$		
r	LDA	B3LYP	HF	LDA	B3LYP	HF
9	−2.10	−1.90	−1.42	0.01	−0.01	−0.03
8	11.47	9.43	6.27	0.52	0.38	0.13
7	6.97	6.29	5.11	−0.37	−0.29	−0.20
6	3.37	2.45	1.24	−0.90	−0.62	−0.19
5	−2.24	−1.72	−1.39	1.87	1.61	1.05
4	1.97	2.06	1.92	−0.27	−0.30	−0.39
3	−6.68	−5.95	−5.04	0.56	0.47	0.38
2	−6.01	−6.58	−6.88	−0.41	−0.51	−0.57
1	0.50	0.37	0.07	−0.09	−0.01	0.09

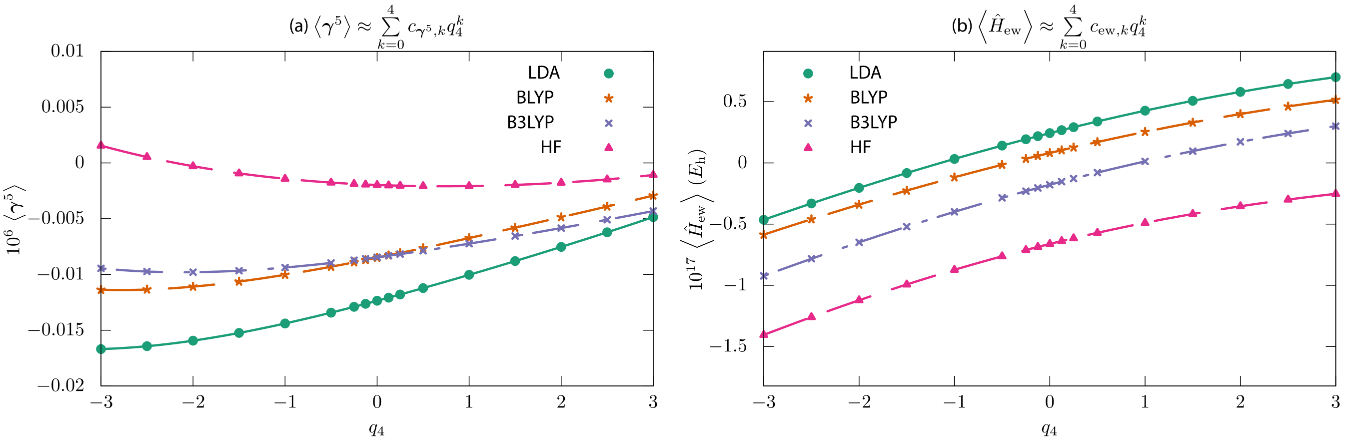

FIG. 5. Dependence of the expectation values of (a) $\boldsymbol{\gamma}^5$ and (b) $\hat{H}_{\mathrm{ew}}$ on the C-F stretching normal coordinate q_4 in (S)-CHBrClF computed at the level of ZORA-cGHF and ZORA-cGKS with different exchange-correlation functionals (points) and polynomial fits to the $\langle\hat{H}_{\mathrm{ew}}\rangle$ and $\langle\boldsymbol{\gamma}^5\rangle$ to fourth order (lines). The results for $\hat{H}_{\mathrm{ew}}$ are a recalculation of those presented in Ref. [67] and are thus identical to those.

Hartree-Fock approach for this property and give again similar results as MP2, we are lead to a rough error estimate of about 30% for the density functionals. Of the different functionals, we give herein tentative preference to the B3LYP results as (i) the absolute values at the equilibrium structures for electroweak $\mathcal{P}$-violation were for B3LYP closer to the MP2 and CCSD(T) values [90,91], (ii) the atomic contributions studied in Refs. [90,91], which are differently weighted by $\langle\boldsymbol{\gamma}^5\rangle$ as compared to $\langle\hat{H}_{\mathrm{ew}}\rangle$, were found to be more consistent with MP2 and CCSD(T) values, and (iii) the vibrational splitting on the B3LYP level is smaller than for the other functionals, which results in more conservative sensitivity estimates.

2. *Sensitivity to static cosmic fields*

The expectation values of $\boldsymbol{\gamma}^5$ and splittings between enantiomers are given in Table IV. As discussed above, we expect multimode effects of the same size as single-mode effects and at the present stage are not able to set upper bounds on b_0^{e} from the CHBrClF experiment. In Ref. [1], we rather estimated the sensitivity of this experiment. Assuming B3LYP to give the best performance (see discussion above), $\Delta_{(R,S)}\langle\boldsymbol{\gamma}^5\rangle$ is on the order of 10^{-10} [$O(10^{-10})$].

The sensitivity of the CHBrClF experiment, performed by Daussy *et al.* in 1999 [46], to b_0^{e} was in Ref. [1] estimated from the experimental upper bound of the $\mathcal{P}$-odd frequency splitting in the C-F stretching fundamental $|\Delta\nu| = 12.7\,\mathrm{Hz}$ [46] as

$$|b_0^{\mathrm{e}}| \lesssim \left|\frac{12.7\,\mathrm{Hz}}{O(10^{-10})}h\right| \sim O(10^{-12}\,\mathrm{GeV})\,. \qquad (44)$$

In comparison to the actual best direct limits on b_0^{e} from modern atomic experiments, that are 2×10^{-14} GeV from Cs and 7×10^{-15} GeV from Dy [30], the 1999 CHBrClF experiment is less sensitive by about two orders of magnitude [1]. However, it is as sensitive as atomic experiments with Tl and Yb ($|b_0^{\mathrm{e}}| < 2 \times 10^{-12}$ GeV; see Ref. [30]).

As emphasized in the discussion of multimode effects, the sensitivity of future experiments can be increased by an order of magnitude when choosing favorable vibrational transitions. As we pointed out in Ref. [1], it was emphasized in Refs. [93,98,99] that the sensitivity of the experiment discussed above is improvable by at least two orders of magnitude by experimental refinement. A choice of a more favorable molecule is expected to lead to further enhancement by two orders of magnitude. Thus, it was estimated in Ref. [1] that in future $\mathcal{P}$-violation experiments with chiral molecules the limits from the 1999 experiment can be improved down to 10^{-17} GeV, i.e., an improvement of the actual best limit by at least two orders of magnitude. This makes experiments with chiral molecules highly powerful tools to search for Lorentz invariance violation beyond the standard model of particle physics.

The accuracy of the estimate for cosmic field effects in CHBrClF, which was in this work indirectly inferred by comparison to previous studies on electroweak $\mathcal{P}$ violation, can in principle be benchmarked by future explicit calculations with systematically improvable electron correlation methods and the presently neglected multimode contributions can be accounted for by explicit calculation of anharmonicity constants. As the main purpose of the present studies was to explore the general potential of chiral molecules to act as sensitive probes for new physics, more accurate theoretical estimates specifically for CHBrClF do not seem to be pressing until new experiments with higher accuracy are performed. Given the pronounced scaling with nuclear charge that was shown analytically and confirmed numerically in this paper, the main focus will likely be shifted to accurate estimates for chiral compounds with heavier elements. Furthermore, our study showed that care has to be taken by choice of the vibrational mode, which on the one hand can directly influence the sensitivity by an order of magnitude and on the other hand can be crucial for accurate theoretical predictions, which are essential to provide limits on cosmic fields from experiments.

V. CONCLUSION AND OUTLOOK

In this paper, we have shown that interactions of electrons with the timelike component of pseudovector cosmic fields are strongly pronounced in chiral molecules. Because of the $\mathcal{P}$-odd contributions of the nuclear potential that electrons experience in a chiral molecule, these interactions lead to $\mathcal{P}$-odd resonance frequency splittings between enantiomers, similar to those from electroweak $\mathcal{P}$-violating interactions. We could show analytically and numerically that these interactions are strongly enhanced in heavy-element-containing molecules and are dominated from contributions that stem from the region near the nucleus. It was demonstrated that $\mathcal{P}$-odd interactions of electrons with cosmic fields behave similarly to interactions due to an electroweak coupling of electrons and nucleons in chiral molecules. Thus, knowledge from electroweak quantum chemistry can be employed to find promising candidate molecules to limit $\mathcal{P}$-odd electronic coupling to cosmic fields. However, care has to be taken as our calculations revealed a stronger dependence of $\boldsymbol{\gamma}^5$ on molecular structure.

We calculated matrix elements of $\mathcal{P}$-odd cosmic field interactions in CHBrClF with quasirelativistic *ab initio* methods, including vibrational corrections, and compared the results of different DFT functionals. Our calculations of $\mathcal{P}$-odd effects along the different normal coordinates of CHBrClF revealed an important role of nonseparable anharmonic effects and showed that the C–F stretching mode in particular is from this perspective not ideally suited for a measurement of $\mathcal{P}$ violation due to cosmic fields. Effects on some other modes are expected to be larger by an order of magnitude. These findings underline the importance to select not only a favorable molecule but also to carefully choose the vibrational transition. However, from our calculations, the sensitivity of a 20-year-old experiment with CHBrClF to $|b_0^{\mathrm{e}}|$ was estimated to be $O(10^{-12}\,\mathrm{GeV})$. This sensitivity is inferior by two orders to the actual best direct measurements drawn from modern atomic $\mathcal{P}$-violation experiments, but was considered to be improvable to the order of $O(10^{-17}\,\mathrm{GeV})$ or better for static pseudovector fields, which would be an improvement of the actually best limit on b_0^{e} by at least two orders of magnitude. This demonstrates the specific virtue that studies on chiral molecules provides in the search for new physics beyond the standard model.

ACKNOWLEDGMENTS

This paper is dedicated to Peter Schwerdtfeger on the occasion of his 65th birthday. The authors are grateful to the Mainz Institute for Theoretical Physics (MITP) for its hospitality and its partial support during the completion of this work. The Marburg team gratefully acknowledges computer time provided by the center for scientific computing (CSC) Frankfurt and financial support by the Deutsche Forschungsgemeinschaft (DFG, German Research Foundation), Projektnummer 328961117, SFB 1319 ELCH. The work of M.G.K. and T.A.I. was supported by the Russian Science Foundation (RSF) Grant No. 19-12-00157.

---

[1] K. Gaul, M. G. Kozlov, T. A. Isaev, and R. Berger, Phys. Rev. Lett. **125**, 123004 (2020).
[2] G. Bertone, D. Hooper, and J. Silk, Phys. Rep. **405**, 279 (2005).
[3] M. Davis, G. Efstathiou, C. S. Frenk, and S. D. M. White, Astrophys. J. **292**, 371 (1985).
[4] S. Dodelson and L. M. Widrow, Phys. Rev. Lett. **72**, 17 (1994).
[5] H.-C. Cheng, J. L. Feng, and K. T. Matchev, Phys. Rev. Lett. **89**, 211301 (2002).
[6] P. Arias, D. Cadamuro, M. Goodsell, J. Jaeckel, J. Redondo, and A. Ringwald, J. Cosmol. Astropart. Phys. 06 (2012) 013.
[7] G. Gentile, P. Salucci, U. Klein, D. Vergani, and P. Kalberla, Mon. Notices Royal Astron. Soc. **351**, 903 (2004).
[8] A. Klypin, A. V. Kravtsov, O. Valenzuela, and F. Prada, Astrophys. J. **522**, 82 (1999).
[9] M. S. Pawlowski, B. Famaey, H. Jerjen, D. Merritt, P. Kroupa, J. Dabringhausen, F. Lüghausen, D. A. Forbes, G. Hensler, F. Hammer, M. Puech, S. Fouquet, H. Flores, and Y. Yang, Mon. Notices Royal Astron. Soc. **442**, 2362 (2014).
[10] J. Kormendy, N. Drory, R. Bender, and M. E. Cornell, Astrophys. J. **723**, 54 (2010).
[11] S. Sachdeva and K. Saha, Astrophys. J. **820**, L4 (2016).
[12] P. Kroupa, B. Famaey, K. S. de Boer, J. Dabringhausen, M. S. Pawlowski, C. M. Boily, H. Jerjen D. Forbes, G. Hensler, and M. Metz, Astron. Astrophys. **523**, A32 (2010).
[13] W. Hu, R. Barkana, and A. Gruzinov, Phys. Rev. Lett. **85**, 1158 (2000).
[14] J.-W. Lee, EPJ Web Conf. **168**, 06005 (2018).
[15] P. W. Graham, D. E. Kaplan, J. Mardon, S. Rajendran, and W. A. Terrano, Phys. Rev. D **93**, 075029 (2016).
[16] R. D. Peccei and H. R. Quinn, Phys. Rev. Lett. **38**, 1440 (1977).
[17] F. Wilczek, Phys. Rev. Lett. **40**, 279 (1978).
[18] S. Weinberg, Phys. Rev. Lett. **40**, 223 (1978).
[19] G. 't Hooft, Phys. Rev. Lett. **37**, 8 (1976).
[20] G. G. di Cortona, E. Hardy, J. P. Vega, and G. Villadoro, J. High Energy Phys. 01 (2016) 034.
[21] H. An, M. Pospelov, J. Pradler, and A. Ritz, Phys. Lett. B **747**, 331 (2015).
[22] R. Catena, K. Fridell, and V. Zema, J. Cosmol. Astropart. Phys. 11 (2018) 018.
[23] D. Colladay and V. A. Kostelecký, Phys. Rev. D **58**, 116002 (1998).
[24] P. W. Graham and S. Rajendran, Phys. Rev. D **84**, 055013 (2011).
[25] P. W. Graham and S. Rajendran, Phys. Rev. D **88**, 035023 (2013).
[26] P. Sikivie, Phys. Rev. Lett. **113**, 201301 (2014).
[27] B. M. Roberts, Y. V. Stadnik, V. A. Dzuba, V. V. Flambaum, N. Leefer, and D. Budker, Phys. Rev. Lett. **113**, 081601 (2014).
[28] Y. V. Stadnik and V. V. Flambaum, Phys. Rev. D **89**, 043522 (2014).
[29] P. W. Graham, D. E. Kaplan, J. Mardon, S. Rajendran, W. A. Terrano, L. Trahms, and T. Wilkason, Phys. Rev. D **97**, 055006 (2018).
[30] B. M. Roberts, Y. V. Stadnik, V. A. Dzuba, V. V. Flambaum, N. Leefer, and D. Budker, Phys. Rev. D **90**, 096005 (2014).
[31] R. Berger and J. Stohner, WIREs Comput. Mol. Sci. **9**, e1396 (2019).

[32] P. Schwerdtfeger, in *Computational Spectroscopy: Methods, Experiments and Applications*, edited by J. Grunenberg (Wiley, Amsterdam, 2010), Chap. 7, pp. 201–221.
[33] M. Quack, J. Stohner, and M. Willeke, Annu. Rev. Phys. Chem. **59**, 741 (2008).
[34] M. Quack and J. Stohner, Chimia **59**, 530 (2005).
[35] J. Crassous, C. Chardonnet, T. Saue, and P. Schwerdtfeger, Org. Biomol. Chem. **3**, 2218 (2005).
[36] R. Berger, in *Relativistic Electronic Structure Theory, Part 2, Applications*, edited by P. Schwerdtfeger (Elsevier, Amsterdam, 2004), Chap. 4, pp. 188–288.
[37] M. Quack, Angew. Chem. Int. Ed. **41**, 4618 (2002).
[38] M. Quack, Chem. Phys. Lett. **132**, 147 (1986).
[39] É. Gajzágó and G. Marx, Atomki Közl. Suppl. **16(2)**, 177 (1974).
[40] V. S. Letokhov, Phys. Lett. A **53**, 275 (1975).
[41] T. Udem, R. Holzwarth, and T. W. Hänsch, Nature (London) **416**, 233 (2002).
[42] M. A. Bouchiat and C. Bouchiat, Eur. Phys. J. D **15**, 5 (2001).
[43] M.-A. Bouchiat, Phys. Rev. Lett. **98**, 043003 (2007).
[44] O. N. Kompanets, A. R. Kukudzhanov, V. S. Letokhov, and L. L. Gervits, Opt. Commun. **19**, 414 (1976).
[45] A. Bauder, A. Beil, D. Luckhaus, F. Müller, and M. Quack, J. Chem. Phys. **106**, 7558 (1997).
[46] C. Daussy, T. Marrel, A. Amy-Klein, C. T. Nguyen, C. J. Bordé, and C. Chardonnet, Phys. Rev. Lett. **83**, 1554 (1999).
[47] J. Vergados and Y. Semertzidis, Nucl. Phys. B **915**, 10 (2017).
[48] V. A. Kostelecký and C. D. Lane, J. Math. Phys. **40**, 6245 (1999).
[49] V. G. Gorshkov, M. G. Kozlov, and L. N. Labzowsky, Zh. Eksp. Teor. Fiz. **82**, 1807 (1982) [Sov. Phys. JETP **55**, 1042 (1982)].
[50] F. Hobi, R. Berger, and J. Stohner, Mol. Phys. **111**, 2345 (2013).
[51] P. Bargueño and I. Gonzalo, Origins Life Evol. B **36**, 171 (2006).
[52] P. Bargueño and R. Pérez de Tudela, Origins Life Evol. B **37**, 253 (2007).
[53] P. Bargueño, A. Dobado, and I. Gonzalo, Europhys. Lett. **82**, 13002 (2008).
[54] R. A. Hegstrom, D. W. Rein, and P. G. H. Sandars, J. Chem. Phys. **73**, 2329 (1980).
[55] M. G. Kozlov and V. I. Kopp, Vestn. Leningrad. Univ., Fiz. Khim. **16**, 120 (1982).
[56] B. Y. Zel'dovich, D. B. Saakyan, and I. I. Sobel'man, Pis'ma Zh. Eksp. Teor. Fiz. **25**, 106 (1977) [JETP Lett. **25**, 94 (1977)].
[57] C. van Wüllen, Z. Phys. Chem. **224**, 413 (2010).
[58] R. Berger, N. Langermann, and C. van Wüllen, Phys. Rev. A **71**, 042105 (2005).
[59] R. Berger and C. van Wüllen, J. Chem. Phys. **122**, 134316 (2005).
[60] S. Nahrwold and R. Berger, J. Chem. Phys. **130**, 214101 (2009).
[61] T. A. Isaev and R. Berger, Phys. Rev. A **86**, 062515 (2012).
[62] K. Gaul and R. Berger, J. Chem. Phys. **147**, 014109 (2017).
[63] K. Gaul and R. Berger, J. Chem. Phys. **152**, 044101 (2020).
[64] R. Ahlrichs, M. Bär, M. Häser, H. Horn, and C. Kölmel, Chem. Phys. Lett. **162**, 165 (1989).
[65] J. K. Laerdahl and P. Schwerdtfeger, Phys. Rev. A **60**, 4439 (1999).
[66] T. H. Dunning Jr., J. Chem. Phys. **90**, 1007 (1989).
[67] R. Berger and J. L. Stuber, Mol. Phys. **105**, 41 (2007).
[68] W. Kohn and L. J. Sham, Phys. Rev. **140**, A1133 (1965).
[69] S. H. Vosko, L. Wilk, and M. Nuisar, Can. J. Phys. **58**, 1200 (1980).
[70] P. A. M. Dirac, Proc. Cambridge Phil. Soc. **26**, 376 (1930).
[71] C. Lee, W. Yang, and R. G. Parr, Phys. Rev. B **37**, 785 (1988).
[72] A. D. Becke, Phys. Rev. A **38**, 3098 (1988).
[73] P. J. Stephens, F. J. Devlin, C. F. Chabalowski, and M. J. Frisch, J. Phys. Chem. **98**, 11623 (1994).
[74] A. D. Becke, J. Chem. Phys. **98**, 1372 (1993).
[75] A. D. Becke, J. Chem. Phys. **98**, 5648 (1993).
[76] C. van Wüllen, J. Chem. Phys. **109**, 392 (1998).
[77] W. Liu, C. van Wüllen, F. Wang, and L. Li, J. Chem. Phys. **116**, 3626 (2002).
[78] L. Visscher and K. G. Dyall, At. Data Nucl. Data Tables **67**, 207 (1997).
[79] L. Wiesenfeld, Mol. Phys. **64**, 739 (1988).
[80] J. N. P. van Stralen, L. Visscher, C. V. Larsen, and H. J. A. Jensen, Chem. Phys. **331**, 81 (2005).
[81] A. Shee, L. Visscher, and T. Saue, J. Chem. Phys. **145**, 184107 (2016).
[82] See Supplemental Material at http://link.aps.org/supplemental/10.1103/PhysRevA.102.032816 for numerical data that is displayed in the various figures of the main text.
[83] M. Senami and K. Ito, Phys. Rev. A **99**, 012509 (2019).
[84] M. Quack and J. Stohner, Phys. Rev. Lett. **84**, 3807 (2000).
[85] M. Quack and J. Stohner, Z. Phys. Chem. **214**, 675 (2000).
[86] J. K. Laerdahl, P. Schwerdtfeger, and H. M. Quiney, Phys. Rev. Lett. **84**, 3811 (2000).
[87] R. G. Viglione, R. Zanasi, P. Lazzeretti, and A. Ligabue, Phys. Rev. A **62**, 052516 (2000).
[88] M. Quack and J. Stohner, Chirality **13**, 745 (2001).
[89] P. Schwerdtfeger, J. K. Laerdahl, and C. Chardonnet, Phys. Rev. A **65**, 042508 (2002).
[90] P. Schwerdtfeger, T. Saue, J. N. P. van Stralen, and L. Visscher, Phys. Rev. A **71**, 012103 (2005).
[91] C. Thierfelder, G. Rauhut, and P. Schwerdtfeger, Phys. Rev. A **81**, 032513 (2010).
[92] T. Marrel, M. Ziskind, C. Daussy, and C. Chardonnet, J. Mol. Struct. **599**, 195 (2001).
[93] M. Ziskind, C. Daussy, T. Marrel, and C. Chardonnet, Eur. Phys. J. D **20**, 219 (2002).
[94] M. Quack and J. Stohner, J. Chem. Phys. **119**, 11228 (2003).
[95] A. D. Buckingham and W. Urland, Chem. Rev. **75**, 113 (1975).
[96] A. Beil, D. Luckhaus, and M. Quack, Ber. Bunsenges. Phys. Chem. **100**, 1853 (1996).
[97] A. Beil, D. Luckhaus, M. Quack, and J. Stohner, Ber. Bunsenges. Phys. Chem. **101**, 311 (1997).
[98] B. Darquié, C. Stoeffler, A. Shelkovnikov, C. Daussy, A. Amy-Klein, C. Chardonnet, S. Zrig, L. Guy, J. Crassous, P. Soulard, P. Asselin, T. R. Huet, P. Schwerdtfeger, R. Bast, and T. Saue, Chirality **22**, 870 (2010).
[99] A. Cournol, M. Manceau, M. Pierens, L. Lecordier, D. B. A. Tran, R. Santagata, B. Argence, A. Goncharov, O. Lopez, M. Abgrall, Y. L. Coq, R. L. Targat, H. A. Martinez, W. K. Lee, D. Xu, P. E. Pottie, R. J. Hendricks, T. E. Wall, J. M. Bieniewska, B. E. Sauer, M. R. Tarbutt, A. Amy-Klein, S. K. Tokunaga, and B. Darquié, Quantum Electron. **49**, 288 (2019).